

**Permission to place a copy of this work on this server  
has been provided by the American Meteorological  
Society. The AMS does not guarantee that the copy  
provided here is an accurate copy of the published  
work.**

## Use of a Rain Gauge Network to Infer the Influence of Environmental Factors on the Propagation of Quasi-Linear Convective Systems in West Africa

JON M. SCHRAGE

*Department of Atmospheric Sciences, Creighton University, Omaha, Nebraska*

ANDREAS H. FINK

*Institute of Geophysics and Meteorology, University of Cologne, Cologne, Germany*

(Manuscript received 7 August 2006, in final form 22 January 2007)

### ABSTRACT

The West African squall line is a key quasi-linear storm system that brings much of the precipitation observed in the data-poor Sudanian climate zone. Squall lines propagate at a wide range of speeds and headings, but the lack of operational radar stations in the region makes quantifying the propagation of the squall lines difficult. A new method of estimating the propagation rate and heading for squall lines is proposed. Based on measurements of the time of onset of precipitation (OOP) at a network of rain gauge stations, an estimate of the propagation characteristics of the squall line can be inferred. By combining estimates of propagation rate with upper-air observations gathered at a nearby radiosonde station, the impact of various environmental factors on the propagation characteristics of West African squall lines is inferred. Results suggest that the propagation speed for West African squall lines is related to the conditions at midtropospheric levels, where dry air and an enhanced easterly flow favor faster propagation. Northerly anomalies at these levels are also associated with faster propagation. When applied to West African squall lines, the correlations between these environmental factors and the speed of propagation are significantly higher than those of methods developed for mesoscale convective systems in other parts of the world.

### 1. Introduction

Westward-propagating squall lines produce much of the observed precipitation in sub-Saharan West Africa. Their contribution to the total rainfall varies significantly with respect to latitude, accounting for as much as 80%–90% of the annual rainfall in the Sahelian climate zone (12°–18°N) (Dhonneur 1981; Mathon et al. 2002a). In the wetter climate zones to the south, squall lines account for about half of the rainfall in the Sudanian climate zone (9°–12°N) (Eldridge 1957; Omotosho 1985) and as little as 16%–32% along the Guinea coast (Acheampong 1982; Omotosho 1985).

Hamilton and Archbold (1945) presented a compelling, early description of these systems. They stated that West African squall lines propagate to the west-southwest at speeds of 25–30 mi h<sup>-1</sup> (11.2–13.4 m s<sup>-1</sup>).

In that study, the severe aspects of squall lines were emphasized, especially the heavy rainfall (often 60 mm h<sup>-1</sup>), reduced visibility (typically 100–200 m), frequent lightning, and strong leading gust front (with winds often in excess of 25 m s<sup>-1</sup>). Furthermore, these systems and their associated gust fronts can loft dust and transport it great distances (e.g., Tetzlaff and Peters 1986).

West African squall lines exhibit a number of structures that have been documented in several studies (e.g., Fortune 1980; Roux et al. 1984; Chong et al. 1987; Roux 1988; Chong and Hauser 1989; Redelsperger et al. 2002). Some of the key features in the precipitation can be seen in Fig. 1, which presents estimates of rain rate in four selected squall lines occurring during the 2002 summer monsoon season, based on overflights of the Tropical Rainfall Measuring Mission's (TRMM's) Precipitation Radar (PR). A salient feature of these westward-propagating systems is the heavy precipitation associated with what is known as the leading "convective region" of the squall line (Zipser 1977; Chong et al. 1987). This structure can be either quasi linear or bowed forward moderately. The arrival of the convec-

---

*Corresponding author address:* Jon M. Schrage, Dept. of Atmospheric Sciences, Creighton University, 2500 California Plaza, Omaha, NE 68178.

E-mail: jon@creighton.edu

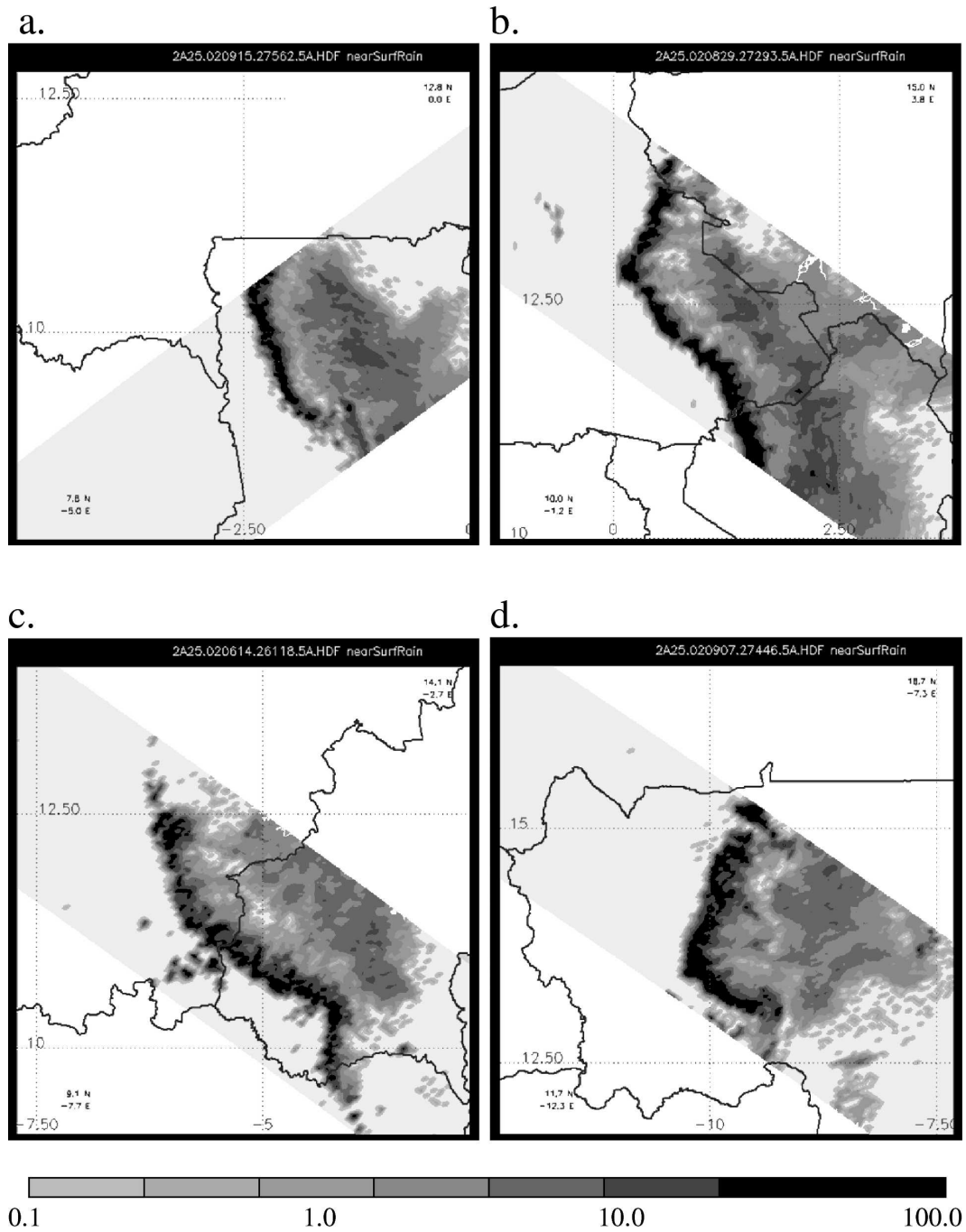


FIG. 1. TRMM PR estimates of "near-surface rain" (mm h<sup>-1</sup>) for squall lines observed on (a) 15 Sep, (b) 29 Aug, (c) 14 Jun, and (d) 7 Sep 2002.

tive region is associated with the passage of the surface gust front and the convective line "leading edge." The leading edge can be understood as a rearward (in terms of the direction of storm motion) sloping plane separating the cloud-free prestorm environment from the towering cumuliform clouds in the convective region (cf. LeMone et al. 1984a, their Fig 2; Barnes and Sieck-

mann 1984). In the present paper, the squall line's arrival will be defined by the onset of precipitation (OOP), which is generally collocated neither with the gust front nor the intersection of the leading edge with the surface. A few tens of kilometers behind the leading edge of the squall line, the precipitation rates fall to near zero in the so-called reflectivity trough (Chong et

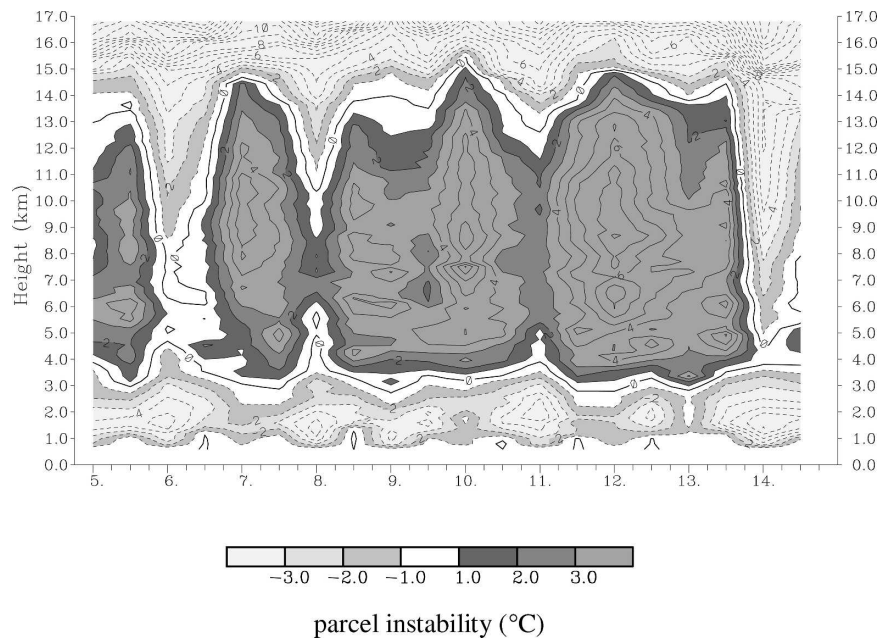


FIG. 2. Parcel instability ( $^{\circ}\text{C}$ ) for Parakou, Benin, in mid-May 2002, expressed in terms of positive and negative temperature differences of a pseudoadiabatically ascending parcel with respect to the ambient air. The starting temperature and humidity values of the parcel were averaged between the surface (i.e., the screen-level observation) and 925 hPa. Negative values suggest CIN and positive values suggest CAPE.

al. 1987). Farther eastward, an irregularly shaped “stratiform region” of precipitation typically extends a few hundred kilometers into the postsquall environment (Zipser 1977; Chong et al. 1987). In situ observations of rain rate have been published in numerous studies (e.g., Sommeria and Testud 1984; Chong et al. 1987; Taylor et al. 1997; Redelsperger et al. 2002; Schrage et al. 2006), which verify this common structure.

Excellent descriptions of the flow in a West African squall line have been presented in several studies, including Roux et al. (1984) and Chong and Hauser (1989). In their analyses, front-to-rear flow in the squall is established as low-level monsoon southwesterlies are lifted by the gust front into the convective region of the storm; the westerly momentum persists at upper-tropospheric levels through the reflectivity trough and the stratiform region, exiting the rear of the system. Additionally, a rear-to-front downdraft is established as midtropospheric easterlies enter the rear of the storm; these easterlies may either be from the large-scale environmental flow or generated locally within this mesoscale system (Smull and Houze 1987). This subsaturated air favors evaporation of hydrometeors in the stratiform region, promoting cooling and subsidence. This rear-to-front downdraft exits the leading edge of the squall line as outflow along a gust front, which is, in

turn, responsible for lifting the inflow into the convective region. The net westward translation of the squall-line system itself also helps create the westerly low-level outflow, as do the downdrafts of the thunderstorms in the convective region, of course. The convective region of the squall line also contributes to the vertical flux of momentum (and, ultimately, the gust front) to an unknown extent over West Africa. For squall lines over the ocean in Global Atmospheric Research Program (GARP) Atlantic Tropical Experiment (GATE), LeMone (1983) and LeMone et al. (1984b) found that the vertical transport of momentum was almost completely generated by processes within the convective region. However, the vertical shear profile and propagation statistics for these systems were substantially different from those over West Africa, and so the applicability of their results to the problem of the generation of the low-level outflow in West African squall lines is unclear.

For the purposes of the present study, two features of the flow are particularly salient: 1) the strong gust front, which is necessary to overcome the substantial convective inhibition (CIN) or negative buoyancy of the West African environment (see Fig. 2), and 2) the evaporative cooling at midtropospheric levels, which provides the mechanism by which easterly momentum is transported to the surface to support the gust front.

Clearly, forecasting the genesis and propagation of such squall lines remains a key issue, both in the research and the operational meteorology communities. Traditionally, measurements of propagation rates are made using radar (e.g., Gamache and Houze 1982). However, in much of West Africa, such facilities do not exist, except in the cases of field experiments (e.g., Chong et al. 1987; Redelsperger et al. 2002). The present study proposes a method to infer the propagation characteristics of squall lines from a dataset based on a network of recording rain gauges. Such networks do exist in West Africa, such as the one described in section 2a.

Section 2 documents the rain gauge network database and the data collected by a special radiosonde station at Parakou, Benin, operated by the Integrated Approach to the Efficient Management of Scarce Water Resources in West Africa (IMPETUS) program. The algorithm used to infer the propagation rate and heading is described in section 3. The distribution of propagation rates and headings, as estimated for the 2002 West African monsoon, is given in section 4. Section 5 then presents results of correlation studies between the propagation characteristics and the vertical profiles of various environmental factors. In section 6, methods developed to forecast the propagation of mesoscale convective systems (MCSs) in other parts of the world are assessed for their applicability to West Africa. Results are summarized in section 7.

## 2. Primary data sources

### a. Observations of time of OOP

A network of 50 recording rain gauges—or “pluviographs”—has been established in the upper Ouémé valley (UOV) of central Benin by the French African Monsoon Multidisciplinary Analyses/Couplage de l’Atmosphère Tropicale et du Cycle Hydrologique (AMMA/CATCH) project and the German IMPETUS project. These pluviographs are distributed unevenly across the 20 000 km<sup>2</sup> of the UOV (Fig. 3), but not all of them were functional throughout the entire 2002 rainy season. However, about 80% of these stations were functioning during the main phase of the monsoon. Thirty-two of these stations were tipping-bucket rain gauges that respond to precipitation amounts of 0.5 mm. As shown in Schrage et al. (2006), rain rates in the convective regions of West African squall lines are typically about 30 mm h<sup>-1</sup> or higher, suggesting that the tipping-bucket rain gauges should discern the OOP within about 1 min from the first rain. The remaining 18 stations featured weighing rain gauges with a rain-rate resolution of 0.1 mm min<sup>-1</sup>; as rain rates in the leading

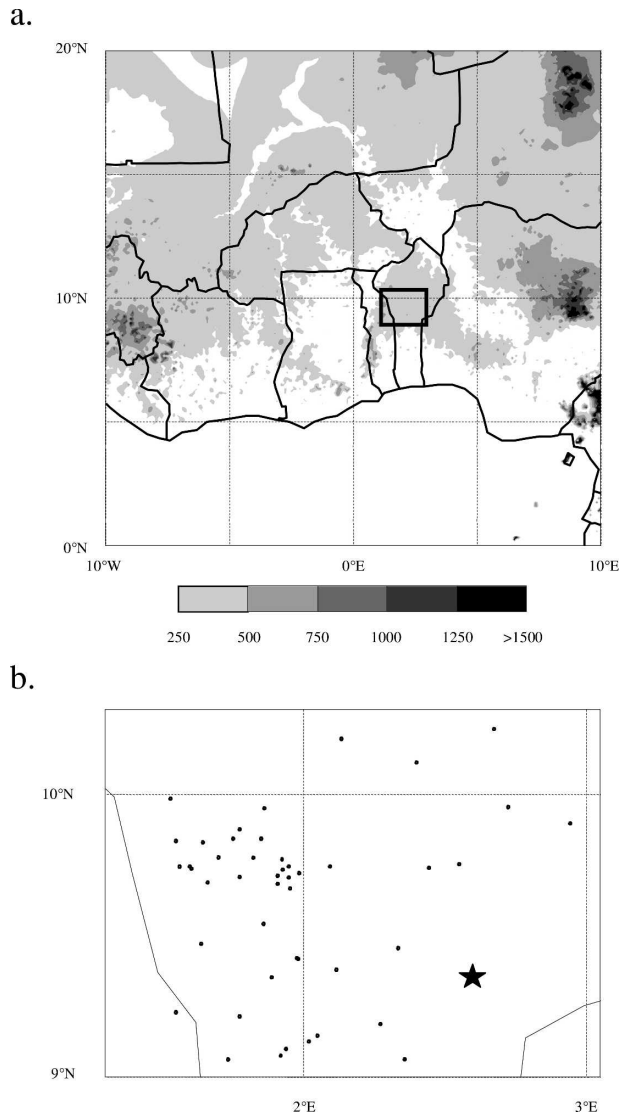


FIG. 3. (a) Topography (m) of central West Africa. (b) Locations of pluviographs in the UOV of Benin (dots), with the radiosonde station at Parakou indicated by a star.

convective region of squall lines are at least a factor of 5 greater than the resolution, the weighing rain gauges also should be able to determine the OOP within about 1 min from the first rains.

For the rainy season of 2002, Fink et al. (2006) used a combination of Meteosat infrared data, wind profiles from radiosonde data, and observations from the rain gauge network to classify precipitation events in the UOV. In particular, they tracked and identified cloud systems based on the configuration of the 233-K brightness temperature isotherm. They identified several different precipitation regimes, the most relevant to the present work being their type Ia, which they described as “advective organized convective systems.” The sys-

TABLE 1. Summary of 31 cases of apparent West African squall lines.

Approx time of OOP in the UOV	Time of sounding at Parakou, Benin	Time between sounding and OOP (h)	$v_{LS}$	$h_{LS}$
1300 UTC 13 Apr 2002	1200 UTC 13 Apr 2002	1	25	90
0300 UTC 9 May 2002	0000 UTC 9 May 2002	3	16.1	120
1900 UTC 12 May 2002	1200 UTC 12 May 2002	7	12.9	20
0700 UTC 19 May 2002	0000 UTC 19 May 2002	7	17.5	20
0400 UTC 24 May 2002	0000 UTC 24 May 2002	4	13.2	90
2200 UTC 26 May 2002	1200 UTC 26 May 2002	10	9.5	155
0600 UTC 28 May 2002	0000 UTC 28 May 2002	6	18.7	95
0400 UTC 1 Jun 2002	0000 UTC 1 Jun 2002	4	24.2	45
1800 UTC 2 Jun 2002	1200 UTC 2 Jun 2002	6	12.7	105
2000 UTC 6 Jun 2002	1200 UTC 6 Jun 2002	8	24.3	35
0300 UTC 13 Jun 2002	0000 UTC 13 Jun 2002	3	18.7	110
0500 UTC 14 Jun 2002	0000 UTC 14 Jun 2002	5	9.8	20
1000 UTC 16 Jun 2002	0000 UTC 16 Jun 2002	10	14.1	70
2200 UTC 20 Jun 2002	1200 UTC 20 Jun 2002	10	15	130
0400 UTC 27 Jun 2002	0000 UTC 27 Jun 2002	4	18	95
2200 UTC 1 Jul 2002	1200 UTC 1 Jul 2002	10	17.7	60
0500 UTC 6 Jul 2002	0000 UTC 6 Jul 2002	5	14.6	105
0800 UTC 9 Jul 2002	0000 UTC 9 Jul 2002	8	11	60
1200 UTC 11 Jul 2002	0000 UTC 11 Jul 2002	12	14.7	60
0300 UTC 12 Jul 2002	0000 UTC 12 Jul 2002	3	24.3	150
1000 UTC 16 Jul 2002	0000 UTC 16 Jul 2002	10	10.7	90
0700 UTC 14 Aug 2002	0000 UTC 14 Aug 2002	7	25.2	45
2000 UTC 16 Aug 2002	1200 UTC 16 Aug 2002	8	15.5	80
2000 UTC 3 Sep 2002	1200 UTC 3 Sep 2002	8	13.6	-10
1000 UTC 11 Sep 2002	0000 UTC 11 Sep 2002	10	9.4	35
0500 UTC 13 Sep 2002	0000 UTC 13 Sep 2002	5	13.6	30
0500 UTC 15 Sep 2002	0000 UTC 15 Sep 2002	5	15.1	100
0400 UTC 18 Sep 2002	0000 UTC 18 Sep 2002	4	18.1	85
0100 UTC 19 Sep 2002	0000 UTC 19 Sep 2002	1	15.4	10
2100 UTC 21 Sep 2002	1200 UTC 21 Sep 2002	9	18.8	70
1200 UTC 24 Sep 2002	0000 UTC 24 Sep 2002	12	20.4	65

tems were “advective” in the sense that they formed outside of the UOV domain and propagated into the UOV not less than 2 h after forming. The term “organized convective system” was defined by Mathon et al. (2002b) and uses infrared satellite-derived statistics to formally specify the size, minimum lifetime, and propagation rate of the cloud cluster. Fink et al. (2006) assumed for their analysis that most of the 52 type Ia systems they tracked over central and western North Africa in the rainy season of 2002 were actually classical West African squall lines at some stage of their lifetime.

The present study used data from the rain gauge network to construct isochrones of time of OOP. Based on these analyses, 21 of the type Ia systems identified by Fink et al. (2006) were found to be inconsistent with the notion of a leading band of heavy, convective precipitation. This difference is not surprising because the classification using satellite data yields a broader geographical picture, whereas the ground-based categorization gives a local perspective of the cloud system. For example, several of these 21 systems were preceded by

local scattered showers, making it difficult to ascertain the appropriate time of OOP for the squall line. Other type Ia cases likely exhibit squall-line characteristics outside the UOV, or affect as a squall system only a small number of stations within the domain. Omitting these 21 type Ia storms, the remaining 31 type Ia systems did exhibit propagation characteristics in their isochrone analyses consistent with the expected structure. A list of these 31 cases is provided in Table 1.

#### *b. Upper-air observations from Parakou, Benin*

The vertical profiles of temperature, humidity, pressure, and wind that were collected during the summer of 2002 by the IMPETUS radiosonde campaign at Parakou (9°21'N, 2°37'E) are a unique dataset for studying the vertical structure of the atmosphere before rainfall events in the Sudanian zone. These observations were made twice daily (0000 and 1200 UTC) at 10-m vertical resolution. At the time of the IMPETUS field campaign in 2002, this station was the only operational ra-

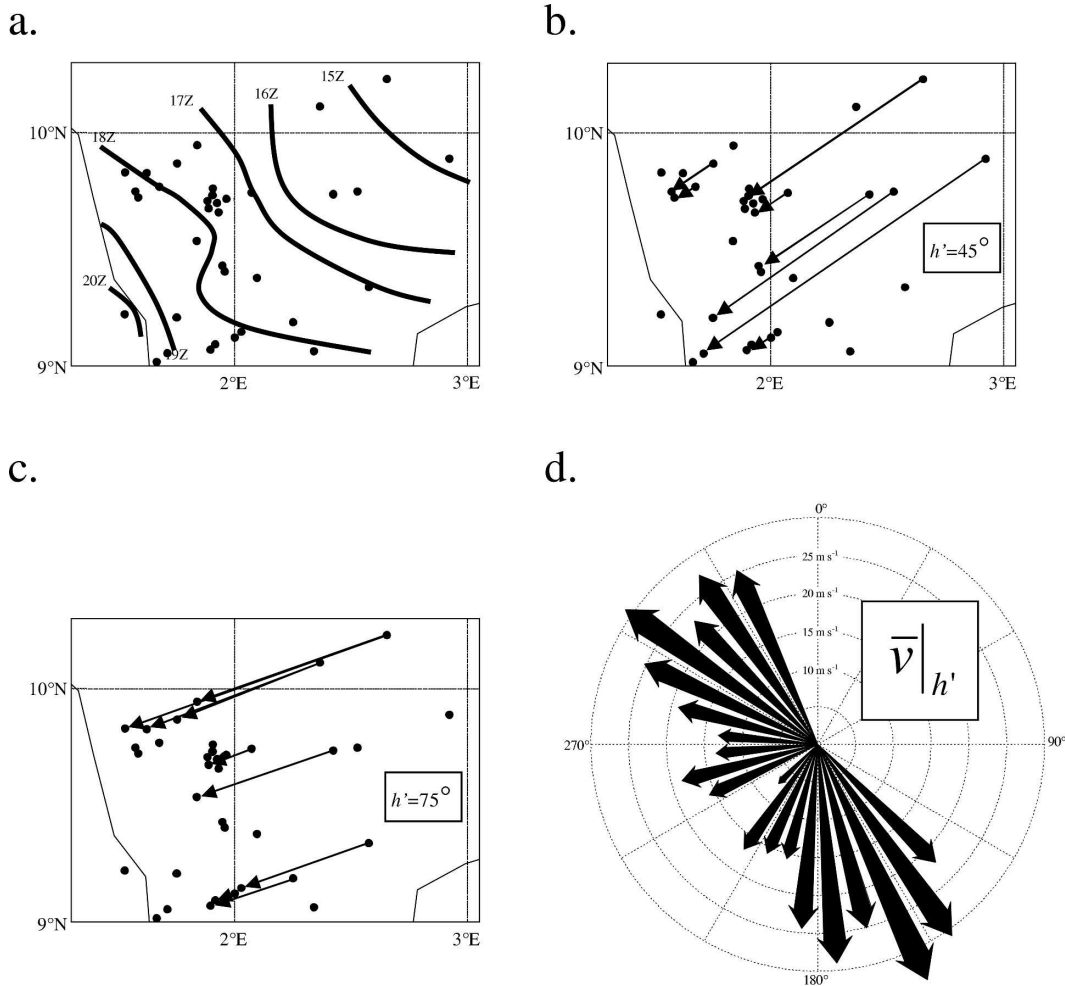


FIG. 4. An illustration of the algorithm used to determine  $\bar{v}|_{h'}$ . Stations that reported precipitation at a realistic time [based on hand analysis of isochrones of OOP, shown in (a)] on 16 Aug 2002 are indicated with dots in (b) and (c). For each arbitrary heading  $h'$  between  $0^\circ$  and  $360^\circ$ , pairs of stations lying along this heading were identified [as suggested by the arrows in (b) and (c)], and an estimate of the propagation speed of the squall line along this heading was determined by averaging the speeds of the squall lines obtained from each pair of stations. (d) The resulting array of speeds.

diosonde station in the Sudanian climate zone of West Africa.

### 3. Inference of speed and heading of squall lines

For each of the 31 precipitation systems, isochrones of the time of the OOP were drawn by hand, such as those shown in Fig. 4a. This analysis helped greatly in the identification of individual stations with outlying observations of OOP, often due to isolated showers earlier in the day or stations that recorded no precipitation associated with the convective region of the squall-line system. Stations with significantly outlying observations of OOP for a given storm were excluded from that storm's analysis.

For all possible combinations of stations  $i$  and  $j$  in the rain gauge network, there exists a distance  $d_{ij}$  and a heading  $h_{ij}$  between these stations. Additionally, all locations have a time  $t_i$  that represents the OOP.

For any arbitrary heading  $h'$ , a certain number of pairs of stations  $i$  and  $j$  are oriented such that their heading  $h_{ij}$  is within some finite range  $\pm\Delta h$  of  $h'$ . Examples of such sets of pairs of stations for two different values of  $h'$  are shown in Figs. 4b,c. In this study, a value of  $5^\circ$  for  $\Delta h$  was found to be adequate. For each of pair of stations, the apparent speed of the squall line between the two stations is computed as

$$v_{ij} = \frac{d_{ij}}{t_j - t_i}. \quad (1)$$

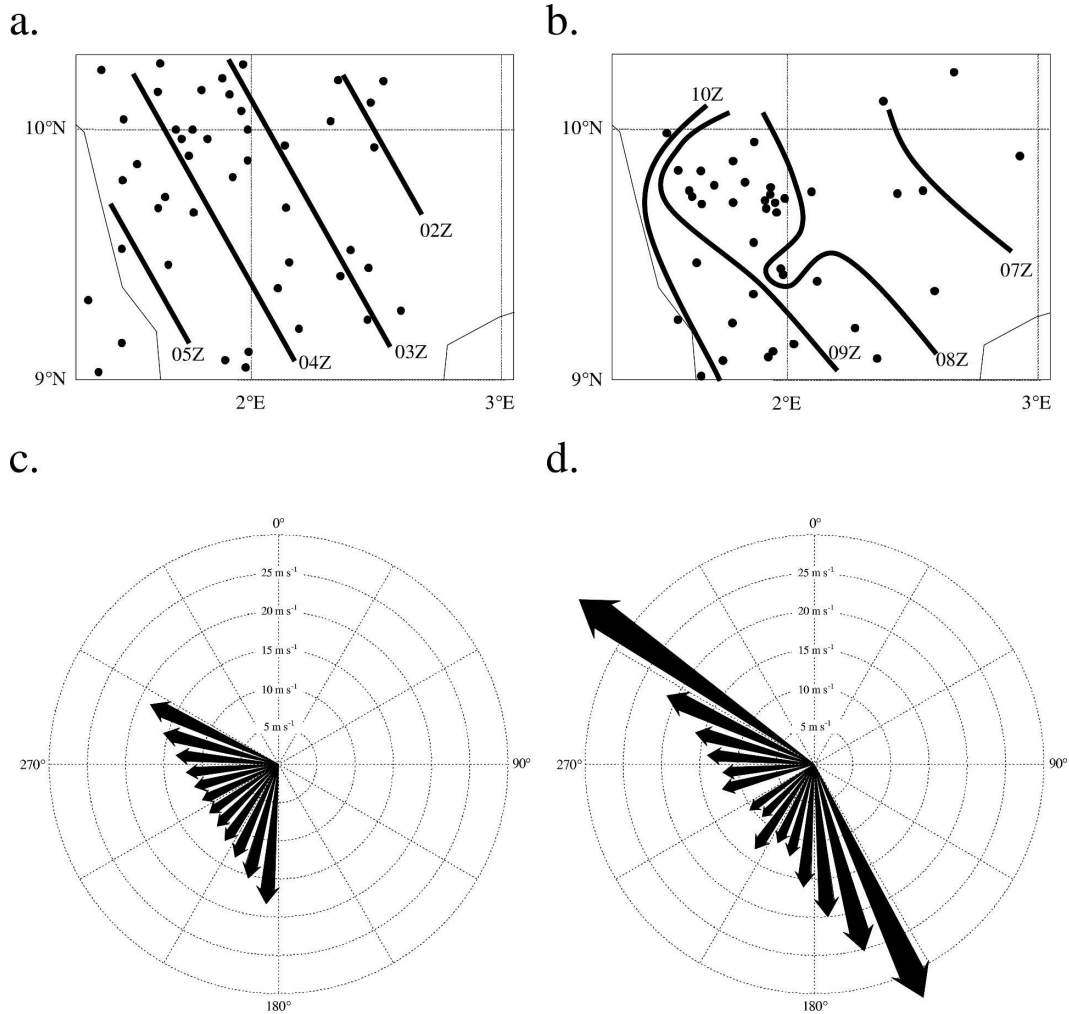


FIG. 5. Isochrones of OOP for (a) an idealized case of synthetic observations and (b) 9 Jul 2002. The computed distributions of  $\bar{v}|_{h'}$  are shown for (c) the idealized case and (d) the observations.

If the denominator of this ratio was small (i.e., stations  $i$  and  $j$  observed nearly the same time for the OOP), the estimates of  $v_{ij}$  were less reliable and more prone to error because of small errors in the observations of the OOP at each station. Therefore, a value of  $v_{ij}$  was only computed if the denominator was at least 600 s. Incidentally, this also had the effect of eliminating pairs of stations that lie along headings roughly perpendicular to the true direction of the propagation of the system, as these pairs of stations tended to observe nearly simultaneous times of OOP despite being separated by great distances.

At the arbitrary heading  $h'$ , therefore, there exists some number of estimates of the velocity of the squall line, based on the pairs of stations that are oriented approximately along the heading  $h'$ . If there were at least three pairs of stations along the given heading

with computed speeds, an average estimate of the velocity along  $h'$  was computed and denoted  $\bar{v}|_{h'}$ . For each squall line, arrays of  $\bar{v}|_{h'}$  were computed for all possible values of  $h'$  from  $0^\circ$  to  $360^\circ$  in  $10^\circ$  increments. These arrays are visualized using rose diagrams such as that shown in Fig. 4d. As described below, there are at least two reasonable methods of estimating the true heading and propagation rate of the squall line, based on these values.

#### a. Heading with minimum propagation rate

From geometry, it can be shown that an estimate of the true heading can be obtained from the data by finding the value of  $h'$  with the lowest value of  $\bar{v}|_{h'}$  for the given case. This approximation can be most readily seen by considering the isochrones (Fig. 5a) and the resulting rose diagram (Fig. 5c) from a fictitious, ideal-



ized case in which a perfectly linear squall line propagates at a constant speed across an observing network. It can be shown by Monte Carlo simulations that these estimates of forward propagation speed are unbiased (unless random errors in the individual observations were unrealistically large). However, this estimate of the forward propagation speed has some properties that make it not an ideal estimator. Most notably, the resulting estimate of propagation rate relied on observations of OOP from an unacceptably small number of stations—in principle, as few as four. Therefore, the estimates of propagation rate were not obtained in this manner. However, this method does illuminate the fact that the estimated propagation rate and heading need to incorporate information from pairs of stations that do not necessarily lie along the true heading of the squall line, as is accomplished in the next section.

#### b. Least squares (LS) propagation rate

On a rose diagram (such as those depicted in Figs. 4d, 5c,d), there is a single point  $(v, h)$  that represents the true speed and heading of the squall line. If the squall line is truly linear and propagating at a constant speed across the observing network, then the endpoints of the vectors on the rose diagram should lie along a straight line that goes through  $(v, h)$  and is perpendicular to a line between  $(v, h)$  and the origin. Therefore, if a line could be fit in an LS manner to the endpoints of the vectors on the rose diagram, the point  $(v_{LS}, h_{LS})$  on this line closest to the origin would be another estimator of the true speed and heading  $(v, h)$  of the squall line. Such an estimator would have the advantage of including data from a large number of pairs of stations in the network, even if these pairs of stations did not lie along the true heading of the squall line.

The location  $(v_{LS}, h_{LS})$  is thus defined as the coordinates that minimize the following function:

$$\frac{1}{n} \sum_{h'=h_{LS}-45^\circ}^{h_{LS}+45^\circ} \left[ \bar{v}|_{h'} - \frac{v_{LS}}{\cos(h' - h_{LS})} \right]^2. \quad (2)$$

Here,  $n$  is the number of headings between  $h_{LS} - 45^\circ$  and  $h_{LS} + 45^\circ$  at which an estimated speed  $\bar{v}|_{h'}$  could be computed. In practice, headings along which the calculated value of  $\bar{v}|_{h'}$  was less than  $3 \text{ m s}^{-1}$  were excluded from the evaluation of (2), as these speeds were deemed unrealistically small for the type Ia (for advective organized convective) systems defined by Fink et al. (2006). This restriction complicates the comparison of the current results with the earlier results of Barnes and Sieckman (1984), in which the very slowest mesoscale cloud lines (i.e., slower than  $3 \text{ m s}^{-1}$ ) were shown to have markedly different environments than the

faster (i.e., faster than  $7 \text{ m s}^{-1}$ ) systems. However, as the purpose of the current study was to explain the variation of propagation speeds within the population of the advective organized convective systems, this restriction was deemed acceptable.

An example of how to define  $(v_{LS}, h_{LS})$  by minimizing (2) is presented in Fig. 6. At all possible coordinates for the location of  $(v, h)$ , the value of (2) is assessed. The summand is just the distance between the endpoint of the vector  $\bar{v}|_{h'}$  and the point on the line that intersects the heading  $h'$  (as suggested by the short, solid lines between the endpoints of the vectors and the line being fit in Fig. 6, where the gray shading indicates the  $\pm 45^\circ$  sector relevant to the computation).

Extensive examination of the estimates of  $(v, h)$  obtained by this LS method demonstrated that the technique yields reliable and reasonable values that appear to be consistent with the large-scale propagation rate suggested by the hand analysis of isochrones of OOP. In particular, Monte Carlo tests were performed to verify that the resulting estimates of squall-line propagation were not sensitive to any potential drift in the clocks at the pluviographs. The results were found to be robust as long as the timing errors were moderate (i.e., less than a matter of minutes) and unbiased.

## 4. Propagation statistics for observed West African squall lines

The values of  $v_{LS}$  and  $h_{LS}$  for 31 convective systems are shown in Table 1. The average estimated speed was  $16.4 \text{ m s}^{-1}$ . The values ranged from  $9.4$  to  $25.2 \text{ m s}^{-1}$ , and the standard deviation was  $4.6 \text{ m s}^{-1}$ . The average heading was  $72^\circ$ . The headings ranged from  $-10^\circ$  to  $155^\circ$ , and the standard deviation was  $41^\circ$ . Comparisons of these values with previous reports of propagation rates for West African squall lines are shown in Table 2.

The timelines of  $v_{LS}$  and  $h_{LS}$  are shown in Fig. 7. There was no significant trend in  $v_{LS}$  over the 2002 rainy season. There was a slight ( $r = -0.281$ ) downward trend to  $h_{LS}$ , with the trendline suggesting that the expected heading of the squall line shifted about  $35^\circ$  to the north between April and late September. The speeds and headings of the systems were uncorrelated with the time of day that the precipitation began in the UOV.

Histograms of  $v_{LS}$  and  $h_{LS}$  are shown in Fig. 8. The distribution of  $v_{LS}$  is in particularly good agreement with the observed distribution of squall-line propagation rates reported by Tetzlaff and Peters (1988), who showed that 15 squall lines during the West African Monsoon Experiment propagated at speeds of  $10$ – $22 \text{ m s}^{-1}$ .

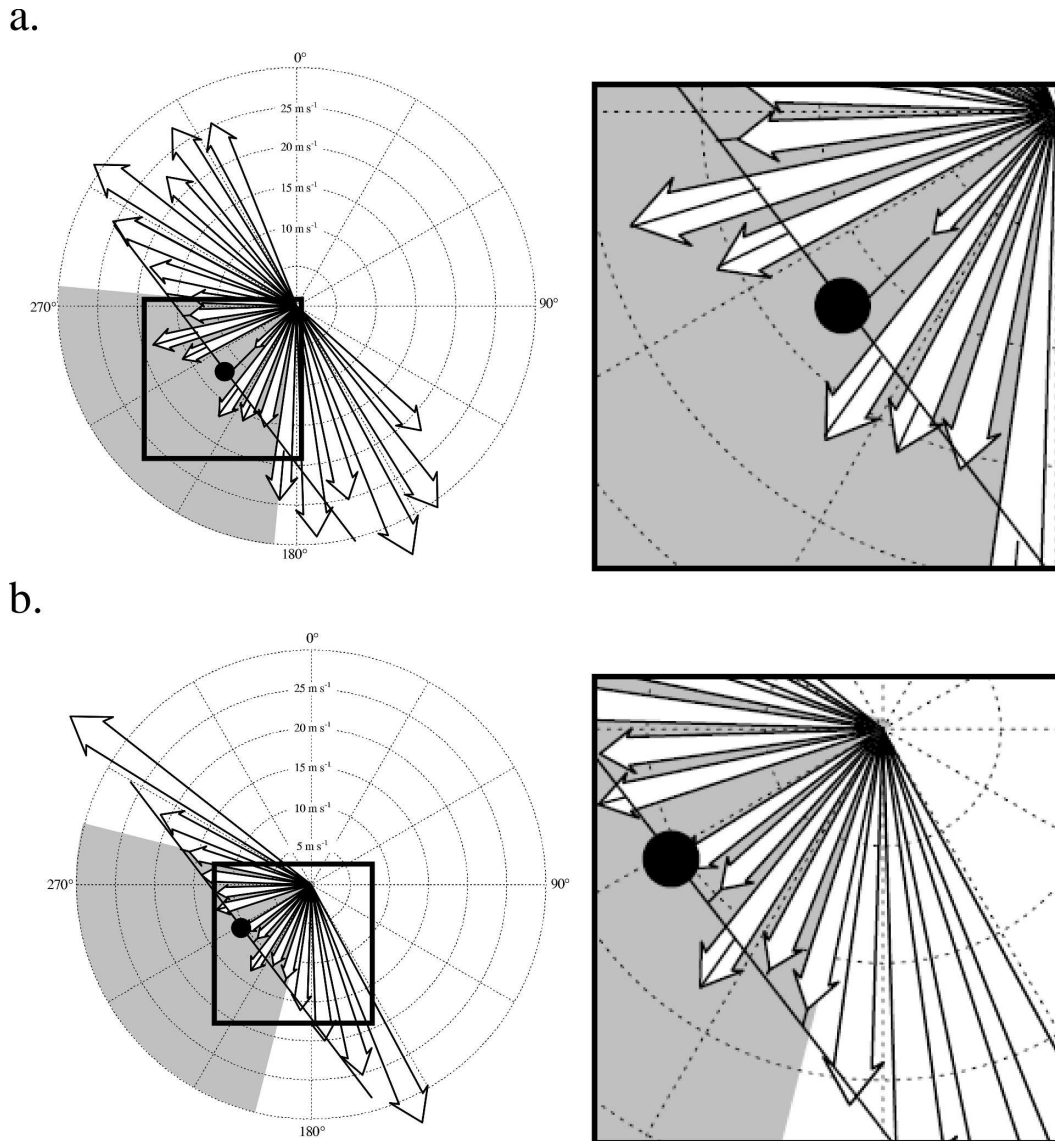


FIG. 6. An illustration of the results of the LS algorithm for (a) 16 Aug and (b) 9 Jul 2002. The panels on the right are enlargements of key sections of the plots on the left. Black circles indicate the locations of  $(v_{LS}, h_{LS})$ , where the function given by (2) is minimized. The corresponding “best fit” lines for the  $\pm 45^\circ$  sectors (shown in gray) are presented, as are the residual errors (solid lines between the tips of the arrows and the best-fit line).

### 5. Influence of the environment on observed propagation characteristics

The operation of the radiosonde station at Parakou, Benin, during the IMPETUS upper-air field campaign provided an opportunity to relate the propagation statistics inferred from the UOV rain gauge network with approximately collocated upper-air observations. For each of the 31 quasi-linear precipitation systems examined, the upper-air observation prior to the OOP was used, as shown in Table 1. On average, these observations were approximately 6.5 h ahead of the OOP, with

none of the upper-air observations being more than 12 h ahead. Considering the configuration of a typical West African squall line, it can be assumed that these soundings reflect the environment ahead of (i.e., to the west of) the precipitation.

The estimates of  $v_{LS}$  were correlated against the corresponding observed profiles of relative humidity, zonal wind, and meridional wind, and the results are shown in Fig. 9. In these diagrams, levels whose correlations reach certain significance thresholds (according to a two-tailed Student’s  $t$  test) are indicated by shading. Altitudes are expressed in kilometers above mean

TABLE 2. Reported squall-line propagation speeds in the literature.

Source	Speed (m s <sup>-1</sup> )	Notes
Current study	16.4	31 systems in 2002
Aspliden et al. (1976)	14–17	During GATE
Bolton (1984)	16.4	27 months, 1974–76
Fernandez (1982)	14.8	3 systems in 1973
Fink and Reiner (2003)	15	344 systems in 1998–99
Fortune (1980)	16–18	1 system, tracked by satellite
Tetzlaff and Peters (1988)	16	15 systems in 1979

sea level; the radiosonde station at Parakou is at an elevation of 393 m.

Significant correlations between  $v_{LS}$  and the relative humidity are seen between 4 and 9 km (Fig. 9a). These negative correlations suggest that that drier (moister) air at midtropospheric levels is associated with a faster (slower) propagation rate. Various authors (e.g., Barnes and Sieckman 1984; Chong et al. 1987; Roux 1988; Peters and Tetzlaff 1988; Peters et al. 1989;

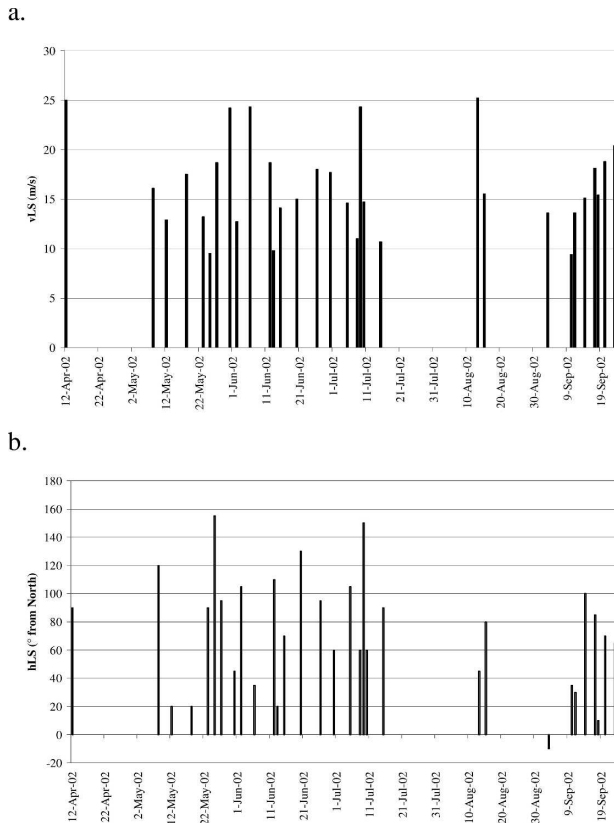


FIG. 7. Timeline of (a) LS propagation speed  $v_{LS}$  and (b) least squares heading  $h_{LS}$  for squall lines during the summer of 2002.

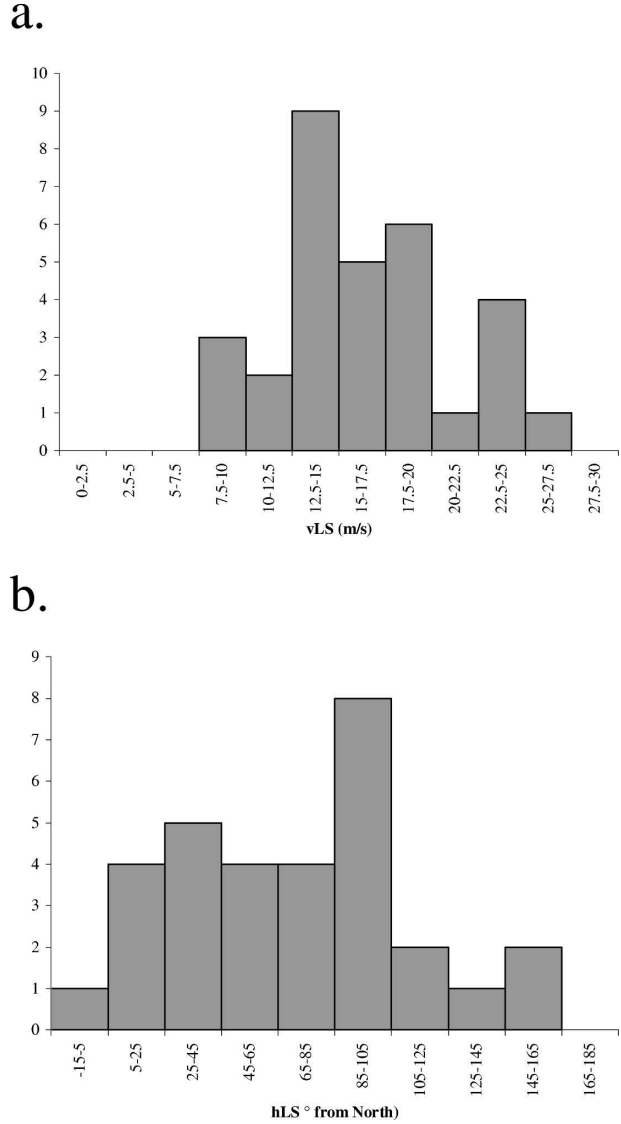


FIG. 8. Histograms of the distribution of (a) the LS propagation rate  $v_{LS}$  and (b) the least squares heading  $h_{LS}$  for the summer of 2002.

Hodges and Thorncroft 1997; Thorncroft et al. 2003) have shown that dry air at these levels leads to evaporation of hydrometeors in both the stratiform and the convective regions of a West African squall line. The resulting cooling helps transport easterly momentum from the midtroposphere down to the surface, contributing to the rear-to-front flow and shear that supports the gust front and its associated nonhydrostatic lifting (e.g., Chong et al. 1987). These correlations suggest that drier (moister) air strengthens (weakens) the rear-to-front downdraft, increasing (decreasing) the forward velocity of the squall-line system.

For the zonal wind (Fig. 9b), the strongest correla-

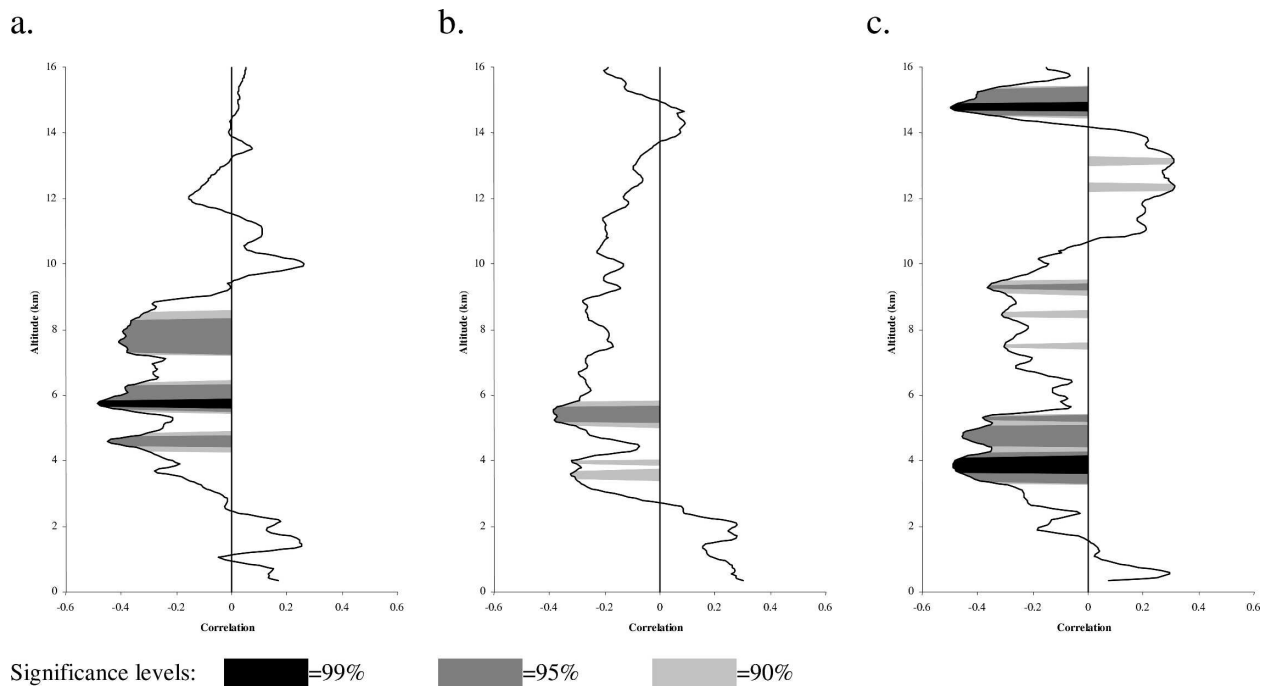


FIG. 9. Correlations between  $v_{LS}$  and profiles of (a) relative humidity, (b) zonal wind, and (c) meridional wind. Altitudes are expressed in km MSL.

tions are seen between about 3.5 and 6 km. Here, negative correlations imply that easterly (westerly) wind anomalies in the midtroposphere are associated with faster (slower) propagation rates. This is again consistent with the notion that the propagation rate for the squall line may be associated with the strength of the rear-to-front downdraft. In the case of enhanced easterly flow, evaporative cooling in the stratiform and convective regions helps transport this excess easterly momentum to the surface, increasing the gust front.

Correlations between the zonal wind component and  $v_{LS}$  (Fig. 9b) in the lowest 2 km were positive but did not reach even the 90% confidence level. However, when the wind vectors were transformed into components “parallel” and “normal” to the leading edge of the squall line, winds normal to the leading edge had somewhat higher correlations ( $r = 0.36$ ) with  $v_{LS}$  (not shown). This suggests that, to a limited degree, the speed of the flow in the monsoon layer influences the rate of propagation of squall lines, with the squall lines actually propagating somewhat faster *upwind* (with respect to flow at the surface) when monsoon flow is enhanced. This is broadly consistent with the Thorpe et al. (1982) analyses that showed that low-level wind shear was necessary feature of squall lines whose source of lifting is their own outflow. Barnes and Sieckman (1984) documented important differences in the roles of components of the flow normal and parallel to the

leading edge of tropical squall lines at several levels of the troposphere, but those results were not confirmed in this analysis, possibly because of the explicit exclusion of the slowest mesoscale cloud lines from the present study.

The correlations between  $v_{LS}$  and the observed meridional winds (Fig. 9c) reveal several deep layers over which the correlations were significant. Very high negative correlations are noted at levels between about 3.5 and 5 km. These negative correlations suggest that northerly (southerly) flow anomalies are associated with faster (slower) propagation rates in the Sudanian climate zone. Aside from the fact that the northerly wind anomalies are presumably advecting dry air southward from the Saharan air layer (SAL; thereby increasing the propagation rate, as noted in Fig. 9a), these strong correlations may also suggest a relationship between the speed of a squall line and the phase of African easterly waves (AEWs). Fink and Reiner (2003) have demonstrated that the association between the phase of AEWs is a function of latitude. South of about  $12.5^{\circ}\text{N}$ , they found that squall lines occur preferentially ahead (i.e., to the west) of the trough axis of the AEW. At these comparatively wet latitudes, they suggested that northerly flow west of the trough axis advects sufficient dry air and midtropospheric levels to produce the necessary evaporative cooling and resulting gust front, which is necessary to overcome the substantial

CIN and negative buoyancy observed in the region (see Fig. 2). The present results suggest that locations west of the trough axis not only favor the existence of squall lines, but also favor faster-propagating system.

The strong negative correlations between  $v_{LS}$  and the meridional wind above 14 km (Fig. 9c) suggest that faster-moving squall lines are associated with northerly wind anomalies in the upper troposphere. By computing correlation coefficients between  $v_{LS}$  and grids of zonal and meridional wind from the European Centre for Medium-Range Weather Forecasts (ECMWF) operational analyses during the summer of 2002 (not shown), it was determined that these northerly winds occur on the southeastern flank of an anomalously strong upper-tropospheric anticyclone centered near 20°N, 10°W. In this analysis, therefore, synoptic conditions that support an especially strong anticyclone aloft apparently also support faster propagation of squall lines in the Sudanian climate zone.

Several authors have noted that propagation of squall lines is related to wind speed at various levels. Bolton (1984) claimed that West African squall lines move slightly faster than the midtropospheric jet stream, Fernandez (1980) showed that squall lines in Venezuela move at approximately the speed of the midlevel environmental wind, and Mansfield (1977) demonstrated that squall lines over water during GATE moved faster than the winds at any tropospheric level. The values of  $v_{LS}$  were significantly correlated ( $r = +0.363$ ) with the observed wind speeds at 650 hPa (i.e., approximately 3.5 km), with  $v_{LS}$  averaging about 3 m s<sup>-1</sup> faster than the winds at this level. At 5.5 km (i.e., the level of highest correlation between  $v_{LS}$  and the zonal wind), the correlation was +0.379 and the squall lines moved about 6 m s<sup>-1</sup> faster than the winds at this level. The mean value of  $v_{LS}$  was approximately equal to the value of the greatest wind speed between 1.5 and 6 km, although the correlations between these parameters were not especially high.

## 6. Existing methods of forecasting propagation

Several previous studies have examined the environmental factors that influence the propagation of MCSs. While generally quite successful for convective systems in the United States, their applicability to West Africa is now assessed. Results are shown in Table 3.

Corfidi et al. (1996) and Corfidi (2003) described vector-based methods of forecasting MCS propagation for upwind- and downwind-propagating systems. Both methods are based on the mean wind vector in the cloud layer (which they define as the 850–300-hPa layer) and the low-level jet vector [which, as in Bonner

TABLE 3. Correlations and biases of other methods of forecasting MCS propagation.

	$v_{LS}$		$h_{LS}$	
	Correlation	Bias (m s <sup>-1</sup> )	Correlation	Bias (°)
Upwind method Corfidi (2003)	0.179	-3.46	0.273	-9°
Downwind method Corfidi (2003)	0.338	4.01	-0.035	-1°
Parallel to thickness contours Merritt and Fritsch (1984)	—	—	0.251	-20°

(1968), was specified as the strongest wind in the lowest 1.5 km]. For the radiosonde observations from Parakou, this “low-level jet” vector was generally found a few hundred meters above ground level and was from the southwest, suggesting that it represented the enhanced monsoon level flow typically seen at night in the region (e.g., Parker et al. 2005). As seen in Table 3, however, neither the upwind nor the downwind methods yielded large and statistically significant correlations. Additionally, the upwind (downwind) method had a bias of -3.46 (4.01) m s<sup>-1</sup> in its estimates of the propagation speed, although the biases in the forecast direction of the systems was quite small for both methods.

Merritt and Fritsch (1984) proposed that MCCs move approximately parallel to contours of 1000–500-hPa thickness. They suggested that the speed of the motion of the systems was related to the relative location of low-level moisture maxima with respect to the convection, which cannot be tested with the current data. To assess the utility of this method for West Africa, grids of 1000–500-hPa thickness were obtained at 1° resolution from the operational version of the ECMWF model. The direction parallel to the thickness contours is at a right angle to the gradient of the thickness. The correlation between the forecasted heading and  $h_{LS}$  was 0.251, with a bias of +20°. This method yielded a fairly narrow range of headings, with over half of the headings being between 85° and 105°. This suggests that the method is not particularly sensitive to the true factors that influence squall-line propagation in West Africa.

Fernandez (1982) reported that a “hydraulic jump analogy” based on the work of Hamilton and Archbold (1945), Freeman (1948), and Tepper (1950) provided good estimates of the propagation speed of three West African squall lines observed during August 1973. Within this framework, a mechanism that produced sudden vertical accelerations below an inversion creates a disturbance in the height of the inversion that propagates as a gravity wave. The associated pressure jump travels at a rate  $C$  given by Fernandez (1982) as

$$C = \left[ gH \left( 1 - \frac{\theta'}{\theta} \right) \right]^{1/2}, \quad (3)$$

where  $g$  is the acceleration of gravity,  $H$  is the height of the temperature inversion,  $\theta'$  is the mean potential temperature below the inversion, and  $\theta$  is the mean potential temperature above the temperature inversion (in practice, for a layer the same thickness as that below the inversion). For the three aforementioned squall lines, Fernandez (1982) used this method to forecast a mean speed of  $11.5 \text{ m s}^{-1}$ , whereas the observed average speed was  $14.8 \text{ m s}^{-1}$ . While those initial results may seem promising, the application of the method to the squall lines from 2002 was unsuccessful. Because the quantity  $\theta'/\theta$  has a very limited range—almost all cases had values between 0.971 and 0.997—the predicted phase speed  $C$  is strongly dependent on  $H^{1/2}$ . While the observed temperature profiles at Parakou all demonstrated temperature inversions, the heights of these inversions varied greatly, from as little as a few hundred meters to as much as 4.1 km above ground level. The resulting estimates of the speed of the squall line, therefore, occurred over an unrealistically large range of values, from about 3 to over  $50 \text{ m s}^{-1}$ . Additionally, the height of the temperature inversion typically fluctuates considerably throughout the course of the day as a result of a number of synoptic and local processes; consequently, the observed height of the temperature inversion a few hours before the arrival of the squall line may not be strongly related to the height at the time of OOP. Thus, the forecast value of this method is limited. The successful use of the method by Fernandez (1982) seems to be related to the small range of values of  $H$  observed in the three storms from 1973.

## 7. Discussion and conclusions

The factors that had the highest correlations with the inferred propagation rates for the squall lines were all interpreted as being related to the magnitude of the rear-to-front flow within the convective system. Smull and Houze (1987) reexamined the results of Chong et al. (1987) for a West African squall line observed by Doppler radar during the Convection Profonde Tropicale 1981 (COPT 81) experiment and concluded that the rear-to-front flow observed in that system had developed locally within the stratiform region due to cloud microphysical processes. They cite Roux et al. (1984) and Roux (1985) as having also noted that the rear-to-front flow was a density current produced in situ in the stratiform region. In this interpretation, the strong negative correlations of  $v_{LS}$  with relative humidity between about 4 and 8 km seem reasonable. At

these levels, the entrainment of dry environmental air into the stratiform cloud layer enhances evaporative cooling and favors the development of this rear-to-front flow.

The robust correlations between  $v_{LS}$  and the zonal wind at about 5.5 km have two possible interpretations. On the one hand, this may represent a kind of “steering level” for the squall line, with mean winds at this level advecting the overall system westward. Alternatively, this may signify the entry of easterly momentum from the environment into the rear of the stratiform region, suggesting that rear-to-front flow itself is stronger in the presence of an environment with enhanced easterlies at midtropospheric levels. Smull and Houze (1987) were not in favor of this latter hypothesis with respect to the squall line observed during COPT 81, although they noted such influxes of environmental air into the rear of stratiform regions in other parts of the world. In contrast, Bolton (1984) claimed that a midtropospheric jet was essential for the formation of a West African squall line, and that the resulting convective system would propagate at a rate slightly higher than the speed of the jet.

The highly significant correlations between  $v_{LS}$  at the meridional winds at about 4 km (or about 625 hPa) suggest that squall lines propagate more rapidly when there are northerly wind anomalies. This level is markedly lower than the levels at which anticorrelations with relative humidity were high, signifying that these meridional winds are not simply advecting dry air southward from the SAL. (Notice that the highest anticorrelations with relative humidity occurred at about 6 km, where the correlations with the meridional wind were near zero.) The altitude of the strong correlations between  $v_{LS}$  and the meridional wind suggests that this represents an influence of AEWs within the African easterly jet (AEJ). The relationship between squall lines and the phase of the AEWs has been examined by many authors (Burpee 1974; Payne and McGarry 1977; Reed et al. 1977; Bolton 1984; Peters and Tetzlaff 1988; Peters et al. 1989; Duvel 1990; Machado et al. 1993; Rowell and Milford 1993; Druyan et al. 1996; Diedhiou et al. 1999; Mathon et al. 2002a; Fink and Reiner 2003) and remains controversial to date. Fink and Reiner (2003) argue that convection and rainfall predominantly occur ahead of the AEW trough in the southern wetter zones of West Africa and that the coupling of AEWs and squall-line systems increases toward the West African coast, which is consistent with the growth of the AEW amplitude. In the present study region close to the Greenwich meridian, AEWs are sometimes ill defined and other synoptic flow patterns may be responsible for midlevel northeasterlies.

For operational meteorologists in West Africa, this research may have useful implications. If a squall line is observed (presumably in satellite imagery) or predicted, these results suggest that a propagation rate faster than the climatological average of approximately  $15 \text{ m s}^{-1}$  should be forecast if the convection is occurring west of the axis of a trough in the AEJ, or if midlevel winds above the mixed layer turned to the northeast, especially if the relative humidities at about 6 km are below about 50%, which was the mean observed relative humidity on days with squall lines. As more radiosonde stations have become operational in years—in large part due to the ongoing efforts of the AMMA community—forecasters will have increased access to the kinds of data that make analyses such as these possible. In particular, with the 6-hourly ascents at Parakou between June and mid-September 2006, it should be possible to overcome one deficiency in the present study (namely, the use of profiles more than 8 h before the arrival of the squall-line system). Having more representative presquall storm environments in the lowest 3 km where wind and humidity fields are influenced by the diurnal cycle may yield more insights into the role of this part of the troposphere on squall-line speed and heading.

*Acknowledgments.* This research is funded by the Federal German Ministry of Education and Research (BMBF) under Grant 01 LW 0301A and by the Ministry of Science and Research (MWF) of the federal state of North Rhine-Westphalia under Grant 313-21200200. The two grants support the IMPETUS project. Partial financial support was provided by NASA ESPCoR via the Nebraska Space Grant, with additional support from the following offices at Creighton University: the Dean of the College of Arts and Sciences, the Dean of the Graduate School, and the Department of Atmospheric Sciences. We are indebted to Volker Ermert, Susan Pohle, and Peggy Reiner for helping us with data processing and graphics production. We are grateful to Christian Depraetere and Jean-Michel Bouchez from the Institut de Recherche pour le Développement for providing us with the AMMA/CATCH rainfall data. Finally, we thank the two anonymous reviewers for their comments, which helped to greatly improve the manuscript.

## REFERENCES

- Acheampong, P. K., 1982: Rainfall anomaly along the coast of Ghana—Its nature and causes. *Geogr. Ann.*, **64A**, 199–211.
- Aspliden, J. P., Y. Tourre, and J. B. Sabine, 1976: Some climatological aspects of West African disturbance lines during GATE. *Mon. Wea. Rev.*, **104**, 1029–1035.
- Barnes, G. M., and K. Sieckman, 1984: The environment of fast- and slow-moving tropical mesoscale convective cloud lines. *Mon. Wea. Rev.*, **112**, 1782–1794.
- Bolton, D., 1984: Generation and propagation of African squall lines. *Quart. J. Roy. Meteor. Soc.*, **110**, 695–721.
- Bonner, W. J., 1968: Climatology of the low-level jet. *Mon. Wea. Rev.*, **96**, 833–850.
- Burpee, R. W., 1974: Characteristics of North African easterly waves during the summers of 1968 and 1969. *J. Atmos. Sci.*, **31**, 1556–1570.
- Chong, M., and D. Hauser, 1989: A tropical squall line observed during the COPT 81 experiment in West Africa. Part II: Water budget. *Mon. Wea. Rev.*, **117**, 728–744.
- , P. Amayenc, G. Scialom, and J. Testud, 1987: A tropical squall line observed during the COPT 81 experiment in West Africa. Part I: Kinematic structure inferred from dual-Doppler radar data. *Mon. Wea. Rev.*, **115**, 670–694.
- Corfidi, S. F., 2003: Cold pools and MCS propagation: Forecasting the motion of downwind-developing MCS. *Wea. Forecasting*, **18**, 997–1017.
- , J. H. Merritt, and J. M. Fritsch, 1996: Predicting the movement of mesoscale convective complexes. *Wea. Forecasting*, **11**, 41–46.
- Dhonneur, G., 1981: Mobile cloud clusters as a principal component of the meteorology of the Sahel (in French). *La Météor.*, **27**, 75–82.
- Diedhiou, A., S. Janicot, A. Viltard, P. de Felice, and H. Laurent, 1999: Easterly wave regimes and associated convection over West Africa and tropical Atlantic: Results from the NCEP/NCAR and ECMWF reanalyses. *Climate Dyn.*, **15**, 795–822.
- Druryan, L. M., P. Lonergan, and M. Saloum, 1996: African wave disturbances and precipitation at Niamey during July–August 1987 and 1988. *Climate Res.*, **7**, 71–83.
- Duvel, J. P., 1990: Convection over tropical Africa and the Atlantic Ocean during northern summer. Part II: Modulation by easterly waves. *Mon. Wea. Rev.*, **118**, 1855–1868.
- Eldridge, R. H., 1957: A synoptic study of West African disturbance lines. *Quart. J. Roy. Meteor. Soc.*, **83**, 303–314.
- Fernandez, W., 1980: Environmental conditions and structure of some types of convective mesosystems observed over Venezuela. *Arch. Meteor. Geophys. Bioklimatol.*, **29A**, 249–267.
- , 1982: Environmental conditions and structure of the West African and eastern tropical Atlantic squall lines. *Arch. Meteor. Geophys. Bioklimatol.*, **31**, 71–89.
- Fink, A. H., and A. Reiner, 2003: Spatiotemporal variability of the relation between African easterly waves and West African squall lines in 1998 and 1999. *J. Geophys. Res.*, **108**, 4332, doi:10.1029/2002JD002816.
- , D. G. Vincent, and V. Ermert, 2006: Rainfall types in the West African Soudanian zone during the summer monsoon 2002. *Mon. Wea. Rev.*, **134**, 2143–2164.
- Fortune, M., 1980: Properties of African squall lines inferred from time-lapse satellite imagery. *Mon. Wea. Rev.*, **108**, 153–168.
- Freeman, J. C., Jr., 1948: An analogy between equatorial easterlies and supersonic gas flow. *J. Meteor.*, **5**, 138–146.
- Gamache, J. F., and J. F. Houze, 1982: Mesoscale air motions associated with a tropical squall line. *Mon. Wea. Rev.*, **110**, 118–135.
- Hamilton, R. A., and J. W. Archbold, 1945: Meteorology of Nigeria and adjacent territory. *Quart. J. Roy. Meteor. Soc.*, **71**, 231–264.
- Hodges, K. I., and C. D. Thorncroft, 1997: Distribution and statistics of African mesoscale convective weather systems

- based on the ISCCP Meteosat imagery. *Mon. Wea. Rev.*, **125**, 2821–2837.
- LeMone, M. A., 1983: Momentum transport by a line of cumulonimbus. *J. Atmos. Sci.*, **40**, 1815–1834.
- , G. M. Barnes, E. J. Szoke, and E. J. Zipser, 1984a: The tilt of the leading edge of mesoscale tropical convective lines. *Mon. Wea. Rev.*, **112**, 510–519.
- , —, and E. J. Zipser, 1984b: Momentum flux by lines of cumulonimbus over the tropical oceans. *J. Atmos. Sci.*, **41**, 1914–1932.
- Machado, L. A. T., J.-P. Duvel, and M. Desbois, 1993: Diurnal variations and modulation by easterly waves of the size distribution of convective cloud clusters over West Africa and the Atlantic Ocean. *Mon. Wea. Rev.*, **121**, 37–49.
- Mansfield, D. A., 1977: Squall lines observed in GATE. *Quart. J. Roy. Meteor. Soc.*, **103**, 569–574.
- Mathon, V. A., A. Diedhiou, and H. Laurent, 2002a: Relationship between easterly waves and mesoscale convective systems over the Sahel. *Geophys. Res. Lett.*, **29**, 1216, doi:10.1029/2001GL014371.
- , H. Laurent, and T. Lebel, 2002b: Mesoscale convective system rainfall in the Sahel. *J. Appl. Meteor.*, **41**, 1081–1092.
- Merritt, J. H., and J. M. Fritsch, 1984: On the movement of the heavy precipitation areas of mid-latitude mesoscale convective complexes. Preprints, *10th Conf. on Weather Analysis and Forecasting*, Clearwater Beach, FL, Amer. Meteor. Soc., 529–536.
- Omotosho, J. B., 1985: The separate contributions of squall lines, thunderstorms and the monsoon to the total rainfall in Nigeria. *J. Climatol.*, **5**, 543–552.
- Parker, D. J., C. D. Thorncroft, R. R. Burton, and A. Diongue-Niang, 2005: Analysis of the African easterly jet, using aircraft observations from the JET2000 experiment. *Quart. J. Roy. Meteor. Soc.*, **131**, 1461–1482.
- Payne, S. W., and M. M. McGarry, 1977: The relationship of satellite inferred convective activity to easterly waves over West Africa and the adjacent ocean during phase III of GATE. *Mon. Wea. Rev.*, **105**, 413–420.
- Peters, M., and G. Tetzlaff, 1988: The structure of West African squall lines and their environmental moisture budget. *Meteor. Atmos. Phys.*, **39**, 74–84.
- , —, and W. Janssen, 1989: Rainfall intensity of West African squall lines. *Ann. Geophys.*, **7**, 227–238.
- Redelsperger, J.-L., A. Diongue, A. Diedhiou, J.-P. Ceron, M. Diop, J.-F. Gueremy, and J.-P. Lafore, 2002: Multi-scale description of a Sahelian synoptic weather system representative of the West African monsoon. *Quart. J. Roy. Meteor. Soc.*, **128**, 1229–1257.
- Reed, R. J., D. C. Norquist, and E. E. Recker, 1977: The structure and properties of African wave disturbances as observed during phase III of GATE. *Mon. Wea. Rev.*, **105**, 317–333.
- Roux, F., 1985: Retrieval of thermodynamic fields from multiple Doppler radar data using the equations of motion and the thermodynamic equation. *Mon. Wea. Rev.*, **113**, 2142–2157.
- , 1988: The West African squall line observed on 23 June 1981 during COPT 81: Kinematics and thermodynamics of the convective region. *J. Atmos. Sci.*, **45**, 406–426.
- , J. Testud, M. Payen, and B. Pinty, 1984: West African squall-line structure retrieved from dual-Doppler radar observations. *J. Atmos. Sci.*, **41**, 3104–3121.
- Rowell, D. P., and J. R. Milford, 1993: On the generation of African squall lines. *J. Climate*, **6**, 1181–1193.
- Schrage, J. M., A. H. Fink, V. Ermert, and E. Alonsou, 2006: Three MCS cases occurring in different synoptic environments in the sub-Saharan wet zone during the 2002 West African monsoon. *J. Atmos. Sci.*, **63**, 2369–2382.
- Sommeria, G., and J. Testud, 1984: COPT 81: A field experiment designed for the study of dynamics and electrical activity of deep convection in continental tropical regions. *Bull. Amer. Meteor. Soc.*, **65**, 4–10.
- Smull, B. F., and R. A. Houze Jr., 1987: Rear inflow in squall-lines with trailing stratiform precipitation. *Mon. Wea. Rev.*, **115**, 2869–2889.
- Taylor, C. M., F. Saïd, and T. Lebel, 1997: Interactions between the land surface and mesoscale rainfall variability during HAPEX-Sahel. *Mon. Wea. Rev.*, **125**, 2211–2227.
- Tepper, M., 1950: A proposed mechanism of squall-lines: The pressure jump line. *J. Meteor.*, **7**, 21–29.
- Tetzlaff, G., and M. Peters, 1986: Deep-sea sediments in the eastern tropical Atlantic off the African coast and meteorological flow patterns over the Sahel. *Geol. Rdschau.*, **75**, 71–79.
- , and —, 1988: A composite study of early summer squall lines and their environment over West Africa. *Meteor. Atmos. Phys.*, **38**, 153–163.
- Thorncroft, C. D., and Coauthors, 2003: The JET2000 project—Aircraft observations of the African easterly jet and African easterly waves. *Bull. Amer. Meteor. Soc.*, **84**, 337–351.
- Thorpe, A. J., M. J. Miller, and M. W. Moncrieff, 1982: Two-dimensional convection in non-constant shear: A model of midlatitude squall lines. *Quart. J. Roy. Meteor. Soc.*, **108**, 739–762.
- Zipser, E. J., 1977: Mesoscale and convective-scale downdrafts as distinct components of squall-line circulation. *Mon. Wea. Rev.*, **105**, 1568–1589.



Copyright of *Weather & Forecasting* is the property of American Meteorological Society and its content may not be copied or emailed to multiple sites or posted to a listserv without the copyright holder's express written permission. However, users may print, download, or email articles for individual use.